Websites:
http://www.sciencepub.net
http://www.sciencepub.net/researcher

Emails:
editor@sciencepub.net
marslandresearcher@gmail.com

Researcher

MARSLAND PRESS
Multidisciplinary Academic Journal Publisher

A Physical Modeling of Waveguide Avalanche Photodiodes With an Undepleted Absorption Layer

S. Nikmanesh*, M. H. Sheikhi**, A. Zahabi ***

* School of Electrical and Computer Eng. Shiraz University
** School of Electrical and Computer Eng. Shiraz University
*** School of Electrical Eng. Islamic Azad University, Bushehr Branch
nikmaneshsamira14@yahoo.com

Abstract: In this paper a theoretical physics-based model of the waveguide avalanche photodiodes is presented. This model is used to calculate both time and frequency responses of this APD's and to investigate the dependence of the multiplication and absorption layer thickness on the 3-dB bandwidths of the waveguide-APD. It is shown that introducing an undepleted absorption layer is effective in improving the 3-dB bandwidth without reducing efficiency. The novelity of this method lies it's high capability in modeling WG-APD with undepleted absorption layer. The gain-bandwidth characteristic of WG-APD is studied for different thicknesses of both the absorption and the multiplication layers. the 3-dB bandwidth of the WG-APD based on the calculation results is over 20 GHz up to a multiplication factor of 7.
[S. Nikmanesh, M. H. Sheikhi, A. Zahabi. **A Physical Modeling of Waveguide Avalanche Photodiodes With an Undepleted Absorption Layer.** *Researcher* 2020;12(3): 60-67]. ISSN 1553-9865 (print); ISSN 2163-8950 (online). http://www.sciencepub.net/researcher. 11. doi:10.7537/marsrsj120320.11.

Keywords: Avalanche photodiodes, frequency response, physics-based modeling, undepleted absorption layer, waveguide-apd

1. Introduction

In recent years, avalanche photodiodes have been used for applications where high receiver sensitivity is required. it is due to their internal gain property [1], [2]. Two important characteristics of a high-performance photo detector are its quantum efficiency and its bandwidth. This two characteristics usually act inverse each other. Waveguide structure (WG-APD) is presented as solution for tradeoff between the band with and quantum efficiency [3], also APD's with a p-type neutral absorption layer (NA-APD's) has been developed by several groups [4]-[8]. Considering the similarity of NA-APD's with unitraveling-carrier photodiode, this structure reduce carrier transit time and don't degrade responsivity [9]. In WG- APD the carrier transport in perpendicular direction to the photon flux and causes the band with and the quantum efficiency are independent each other. With using a wider band gap material for the multiplication layer and a narrow band gap material for the absorption layer achieve a high gain-bandwidth product [10]. For high speed operation and hybrid integration on a planar light wave circuits (PLC), the waveguide structure is an appropriate candidate. so WG-APDs are promising for next generation of high-speed long –distance communication system [11].

In order to improve a maximum 3-dB bandwidth and a GB-product, an undepleted absorption layer which includes a p-type gradient-doped layer was utilized [12].

In this paper a new WG-APD with undepleted absorption layer is analyzed. Also the theoretical calculation of the 3-dB bandwidth of the WG-APD with an undeleted absorption layer is described. The effect of undepleted absorption layer on 3-dB bandwidth was also investigated. The undepleted absorption layer includes a p-type gradient-doped layer. The doping density in the undepleted absorption layer was linearly increasing toward the p -InAlGaAs layer from 5×10^{17} to 2×10^{18} cm^{-3} to form a quasi-electrical field. This layer can reduced the carrier transit time, which is determined ordinarily by slow hole movement, without sacrificing the responsibility. Because of the hole transit time in the p-type gradient-doped layer is dominated by the dielectric relaxation time and negligible.

In addition, the time and frequency responses of the WG-APD with an undepleted absorption layer are developed and presented in section 2 and 3 respectively. For determination the relationships between the performance and design parameters, these time and frequency responses have been studied for different dimensions of the photodetector. The behaviour of the transfer function of this model is discussed, showing the effects of the dimensions of the

photodetector and its multiplication gain. Also the circuit model of the WG-APD consist of all the parasitics of the photodetector is presented in section 4. also we present comparisons of results with the WG-APD without undepleted absorption layer. The results of this physical-modeling are compared to the publish experimental work.

The effects of the dimensions of the photodetectors and the thicknesses of both the absorption and the multiplication layers on its gain-bandwidth characteristics are studied in section 5.

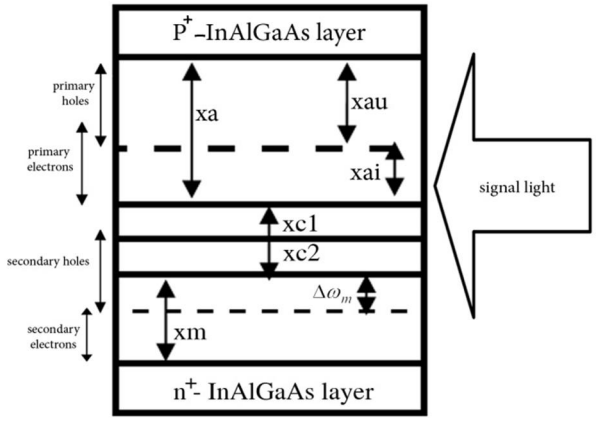

Fig.1.shematic of WG-APD model for calculations

Finally the conclusions are presented in section 6. Also an appendix is added at the end of the paper for easy reference.

2. Time Response of the Photodetector

Time response of the photodetector according to fig.1 the WG-APD structure model for calculations is shown. the primary electron-hole pairs are generated by the lateral incident optical signal on the absorption layer, the structure includes an In AlAs multiplication layer, two step i-InGaAs absorption layer and undepleted InGaAs layer. As the primary electrons travel a dead space length ($\Delta\omega_m$) inside the multiplication generate and they travel to the N^+ layer and P^+ layer under the effect of the electric field. For moving photogenerated carriers at their saturation velocities V_n for electrons and V_p for holes in i-InGaAs layer and V_{p1} for holes undepleted-InGaAs layer the electric field is suppose to be enough high.

For calculating the photocurrent of the WG-APD the time response of this carriers in this analysis be computed. for the primary photo generated electrons $N_p(t)$ and holes $P_p(t)$ are expressed in (1) and (2) respectively.

$$N_P(t)=\eta\frac{p_i}{h\nu}\left\{\left[u(t)-u\left(t-\frac{x_m+x_c}{v_n}\right)\right]+\left(\frac{x_a+x_m+x_c-v_nt}{x_c}\right)\left[u(t-\frac{x_m+x_c}{v_n})-u\left(t-\frac{x_m+x_c+x_a}{v_n}\right)\right]\right\} \quad (1)$$

$$P_p(t)=\eta\frac{P_i}{h\nu}\left\{\left[\frac{x_a-v_pt}{x_a}\right]\left[u(t)-u\left(t-\frac{x_a}{v_p}\right)\right]\right\} \quad (2)$$

Where x_a and x_m are the thicknesses of the absorption and multiplication layer, as they are described in fig.1.

x_i is the total thickness of the charge and the graded layers between the absorption and multiplication layers. First part of (1) explains the generation and drift of the photogenerated electrons. the second part describe that these carriers at the contact of the photodetector. A proof of the time response of primary holes is shown in the appendix.

η is expressed as the quantum efficiency of the waveguide photodetector that can be shown [13].

$$\eta=k(1-R)(1-\exp(-\alpha\Gamma l)) \quad (3)$$

Where K is the coupling efficiency, R is the reflectivity of the photodetector, α is the absorption coefficient of the absorption region, Γ is the confirement factor of the absorption layer, l is the length of absorption layer.

When all the primary electrons traversed the dead space length ($\Delta\omega_m$) of the multiplication layer, they are experiencing lumped multiplication process that cause to generation of the secondary electrons and holes. By convoluting the term exp $[-t/((M_0-1)\tau_m)]/\tau_m$ with the number of the primary electrons that have travelled.

$\Delta\omega_m$ in multiplication layer, the avalanche build up process is achieved. That M_o is the multiplication gain and τ_m is avalanche build up time. [14]

An expressions for the numbers of the secondary generated electrons and holes as a function of time is shown in equations (4), (5).

$$N_S(t) = \eta (M_O - 1)\frac{P_i}{h\nu} \times \left\{ \left(\frac{v_n t - (x_c + \Delta\omega_m)}{x_a} \right) \times \left[u\left(t - \frac{x_c + \Delta\omega_m}{v_n} \right) - u\left(t - \frac{x_m + x_c}{v_n} \right) \right] + \left(\frac{x_m - \Delta\omega_m}{x_a} \right) \left[u\left(t - \frac{x_c + x_m}{v_n} \right) - u\left(t - \frac{x_m + x_c + \Delta\omega_m}{v_n} \right) \right] + \left(\frac{x_a + x_c + x_m - v_n t}{x_a} \right) \times \left[u\left(t - \frac{x_a + x_c + \Delta\omega_m}{v_n} \right) - u\left(t - \frac{x_a + x_c + x_m}{v_n} \right) \right] \right\} \otimes \left\{ \frac{\exp\left(-\frac{t}{(M_O - 1)\tau_m} \right)}{(M_O - 1)\tau_m} \right\}. \quad (4)$$

$$P_s(t) = \eta (M_O - 1)\frac{P_i}{h\nu} \times \left\{ \left(\frac{v_n t - (x_c + \Delta\omega_m)}{x_a} \right) \times \left[u\left(t - \frac{x_c + \Delta\omega_m}{V_n} \right) - u\left(t - \frac{x_{au} + x_{ai} + x_c + \Delta\omega_m}{v_n} \right) \right] + \left[u\left(t - \frac{x_{au} + x_{ai} + x_c + \Delta\omega_m}{V_n} \right) - u\left(t - \left(\frac{x_c + \Delta\omega_m}{v_n} + \frac{x_{ai} + x_c + \Delta\omega_m}{v_p} + \frac{x_{au}}{v_{p1}} \right) \right) \right] + \left(\frac{x_{au}\left(1 + \frac{v_n}{v_{p1}} \right) + (x_{ai} + x_c + \Delta\omega_m)\left(1 + \frac{v_n}{v_p} \right) - v_n t}{x_a} \right) \times \left[u\left(t - \left(\frac{x_c + \Delta\omega_m}{v_n} + \frac{x_{ai} + x_c + \Delta\omega_m}{v_p} + \frac{x_{au}}{v_{p1}} \right) \right) - u\left(t - \left(\frac{x_{ai} + x_{au} + \Delta\omega_m + x_c}{v_n} + \frac{x_{ai} + x_c + \Delta\omega_m}{v_p} \right) \right) \right] \right\} \otimes \left\{ \frac{\exp\left(-\frac{t}{(M_o - 1)\tau_m} \right)}{(M_o - 1)\tau_m} \right\} \quad (5)$$

The time response of the secondary holes is photogenerated in equation (4). the generation of the secondary carriers is expressed by the first term in the first bracket, the drift of these secondary carriers toward the contacts of the photodetector is expressed by the second term while the collection of these carriers is expressed by the third term also expresses the convolution operation. In (5) we suppose that primary holes travel during absorption layer with two different velocities that shown with V_p in i-layer and V_{p1} in undepleted layer. In (5) x_{au} is thickness of the undepleted absorption layer and x_{ai} is thickness of the i-absorption layer.

By using the time respone of the photogenerated carriers and the expression of the photogenerated current the time response of the photocurrent of the photodetector is obtained. I_{ph} the intrinsic photocurrent of device is expressed as (6)

$$I_{ph}(t) = \frac{q}{w_t}\left[v_n\left(N_P(t) + N_s(t) \right) + v_p\left(p_p(t) + p_s(t) \right) \right] \quad (6)$$

Where ω_t is total thickness of photodetector as defined in fig.1.

3. Frequency response of the photodetector

We obtain the frequency response of the photogenerated primary and secondary carriers by calculating the fourier transform of their time responses in (1) - (5). in equation (7)– (10) the frequency responses $N_p(\omega)$, $P_p(\omega)$, $N_s(\omega)$ and $P_s(\omega)$ is expressed. in (10) " m " is multiplication gain factor and dw is □□m in Fig.1.

$$p_p(\omega) = \eta\frac{p_i}{h\nu}\left\{ \frac{1}{j\omega} + \frac{v_p\left(1 - \exp\left(-\frac{j\omega x_a}{v_p} \right) \right)}{x_a\omega^2} \right\} \quad (8)$$

$$N_p(\omega) = \eta\frac{p_i}{h\nu} \times \left\{ \frac{1}{j\omega} + \frac{v_n\left(1 - \exp\left(-\frac{j\omega x_a}{v_n} \right) \right)\exp\left(-\frac{j\omega(x_c + x_m)}{v_n} \right)}{x_a\omega^2} \right\} \quad (7)$$

$$N_s(w) = \eta \frac{p_i}{h\nu}\left(\frac{M_o - 1}{1 + j\omega\tau_m(M_o - 1)}\right).\left(\frac{v_n}{x_a\omega^2}\right)$$

$$.\left[1 - \exp\left(-\frac{j\omega x_a}{v_n}\right)\right].\exp\left(-\frac{j\omega x_c}{v_n}\right)$$

$$.\left[\exp\left(-\frac{j\omega x_m}{v_n}\right) - \exp\left(-\frac{j\omega\Delta\omega_m}{v_n}\right)\right] \qquad (9)$$

$p_s(\omega) = \eta\frac{P_i}{ht}$ {(1/(x_a)) (jv_n ((x_t+$\Delta\omega_m$) (exp (jω((x_t+$\Delta\omega_m$)/v_n)))/(ωv_n)+j (exp (jω ((x_t+$\Delta\omega_m$)/v_n)))/(ω^2)+((x_{au}+x_{ai}+x_t+$\Delta\omega_m$) /($v_n\omega$)) (exp (-jω((x_{au}+x_{ai}+x_t+$\Delta\omega_m$)/v_n)))-(j/($\omega\omega$)) (exp (jω ((x_{au}+x_{ai}+x_t+$\Delta\omega_m$)/v_n)))))-(1/(x_a)) (jv_n (((1/ω) ((x_t+$\Delta\omega_m$)/v_n+(x_{ai}+x_t+$\Delta\omega_m$)/v_p+x_{au}/v_{p1}) (exp (jω((x_t+$\Delta\omega_m$)/v_n+(x_{ai}+x_t+$\Delta\omega_m$)/v_p+x_{au}/v_{p1})))+(j/(ω^2)) (exp (jω((x_t+$\Delta\omega_m$)/v_n+(x_{ai}+x_t+$\Delta\omega_m$)/v_p+x_{au}/v_{p1})))+(1/(ω)) ((x_{au}+x_{ai}+x_t+$\Delta\omega_m$)/v_n+(x_{ai}+x_t+$\Delta\omega_m$)/v_p+x_{au}/v_{p1}) (exp (jω((x_{au}+x_{ai}+x_t+$\Delta\omega_m$)/v_n+(x_{ai}+x_t+$\Delta\omega_m$)/v_p +x_{au}/v_{p1}))) (j/(ω^2)) (exp (jω((x_{au}+x_{ai}+x_t+$\Delta\omega_m$)/v_n+(x_{ai}+x_t+$\Delta\omega_m$)/v_p+x_{au}/v_{p1})))))-((x_t+$\Delta\omega_m$)/(jωx_a)) ((exp (jω((x_t+$\Delta\omega_m$)/v_n))) (exp (jω((x_t+$\Delta\omega_m$+x_{au}+x_{ai})/v_n))))+(1/(jω)) ((exp (jω((x_{au}+x_{ai}+x_t+$\Delta\omega_m$)/vn))) -(exp (jω((x_t+$\Delta\omega_m$)/v_n +(x_{ai}+x_t+$\Delta\omega_m$)/v_p+x_{au}/v_{p1}))))+(1/(j$\omega v_{p1}v_p x_a$)) (($x_{au}v_pv_{p1}$+$x_{au}v_pv_n$+$v_{p1}x_{ai}v_p$+$v_{p1}x_{ai}v_n$+$v_{p1}x_tv_p$+$v_{p1}x_tv_n$+$v_{p1}\Delta\omega_m v_p$+$v_{p1}\Delta\omega_m v_n$) ((exp (jω((x_t+$\Delta\omega_m$)/ v_n+(x_{ai}+x_t+$\Delta\omega_m$)/v_p+x_{au}/v_{p1})))-(exp (jω((x_{au}+x_{ai}+x_t+$\Delta\omega_m$)/v_n+(x_{ai}+x_t+$\Delta\omega_m$)/v_p+x_{au}/v_{p1})))) (M_0-1)/(1+jω(M_0-1)τ_m)};

(10)

By substituting (7) – (10) in fourier transform of equation (6) the frequency response of the photocurrent $I_{ph}(\omega)$ is given by

$$I_{ph}(\omega) = \frac{q\left[v_n\left(N_p(\omega) + N_s(\omega)\right) + v_p\left(p_p(\omega) + p_s(\omega)\right)\right]}{w_t} \qquad (11)$$

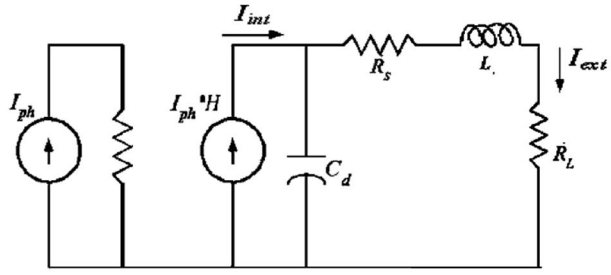

Fig. 2. Equivalent circuit model of the WG-APDs.

4. equivalent circuit model of WG-APDs

In order to the conventional model of PIN-PD presented in [15], [16] and the circuit model of the WG-APD in [17], fig.2. shows the circuit model of this WG-APD. I_{opt} is the optical current and it is given by

$$I_{opt} = \frac{qP_i}{h\nu} \qquad (12)$$

$$H(\omega) = \frac{I_{ph}(\omega)}{I_{opt}(\omega)} = H_s(\omega) + H_p(\omega) \qquad (13)$$

And describe the transfer function (H) according to equation (7) – (11). by (13)

Where Hp and H_S are the primary photogenerations the secondary photogenerations respectively.

The material and the thicknesses of the different layers of the WG-APD are listed in table 1, and the values of the parameters of the photodetector are in the table 2. in fig.3. the transfer function of the circuit model for different values of the multiplication gain is shown in fig.3, we see that the bandwidth of the photodetector decrease for higher multiplication gain (M_0). This happening is because of the avalanche build up process that depands on the value of M_0.

Table 1

Layer	Material	Thickness (nm)
x_a	InGaAs	370
x_{au}	Undepleted-InGaAs	200
x_{ai}	i-InGaAs	170
x_{c1}	InAlGaAs	50
x_{c2}	InAlAs	50
x_m	InAlAs	100

Table 1. Materialas and Thicknesses of the Different Layers of the WG-APD that is presented in [18].

Table 2

Parameter	Value
v_n	$6\times10^6 cm/s$
v_p	$4\times10^6 cm/s$
v_{p1}	$5\times10^6 cm/s$
λ	$1.55\mu m$
ε_r	13.94
α	$1.15\times10^4 cm^{-1}$

Table 2. Parameters of the WG-APD

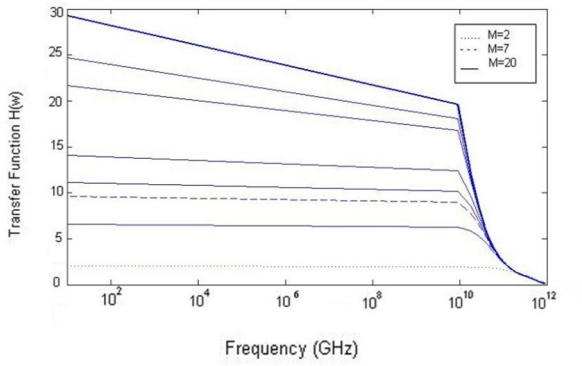

Fig.3. Transfer function of the circuit model for this photodetector.

$$\frac{1}{C_d}=\sum_{j=1}^{No.of\ layers}\frac{1}{Cj},\ where\, C_j=\frac{\varepsilon_o\varepsilon_{rj}A}{x_j} \quad (14)$$

By considering the parasitics of the photodetector in fig.2. Cj is the junction capacitance of the photodetector consist of series capacitances of the different layars that is shown.

Where J is the number of the layers, Cj is layers capacitance that depends on the depleted layer thickness and its area, Rs is contact resistance, L is the pad inductance.

With mixing the photogenerated carriers and the parasitics elements, the extrinsic responcse of the photodetector is expressed as

$$I_{out}(\omega)=I_{opt}H(\omega)H_{\exp}(\omega) \quad (15)$$

$$H_{ext}(\omega)=\frac{1}{1+j\omega C_d R_{tot}-\omega^2 C_d L_s} \quad (16)$$

Where Hext (ω) is the transfer function of the circuit implementation of the parasitic effects of the photodetector as expressed.

The value of R_s, L, R_l that is derivated from experimental paper [18], as shown.

$R_s = 10\ \Omega$ L = 100 pH
$= 50\ \Omega$

5. Effect of the undepleted absorption layer on the bandwidth

In this part, the effect of the undepleted absorption layer on the bandwidth of the photodetector is discussed. When the multiplication factor is low the response time is depended on the carrier transit time in the depleted absorption layer because of using the undepleted absorption layer, the hole traverse the layers with large velocity. The holes in the undepleted layer are the majority carriers and can respond quickly so that the transit time of a hole becomes negligble. The electron transit time needed to get through the layer can be shortened by varying the p-doping concentration along the layer thickness that cause the electron velocity be over shoot. [19], [20]

In this analysis the total absorption layer thickness (x_a) is 0.37 μm and electron overshoot velocity is $2*10^7$ cm/s In undepleted absorption layer [20].

in fig.4. the theoretical 3-dB bandwidth as a function of the undepleted absorption layer thickness (x_{au}) for different multiplication factors is shown. As shown in fig.4. first the 3-dB bandwidth increases by increasing of the undepleted absorption layer then of the (x_{au}) is ~ 0.3 μm the 3-dB bandwidth gradually decreases because the junction capacitance increase for thinner (x_{ai}). ($x_{ai} = x_a - x_{au}$).

Also in fig.4. is shown that the 3-dB bandwidth could be maintained over 20GHz up to a multiplication factor of 7 for WG-APD with a 0.17 – μm-thick i-InGaAs and a 0.20 – μm-thick p-type gradient-doped InGaAs absorption layers. thus this WG-APD can be used for the 25-Gb/s transmission rate up to a M_0=7.

In fig.4. the theoretical 3-dB bandwidth as a function of the undepleted absorption layer thickness x_{au} for different multiplication factors is shown that

firstly the 3-dB bandwidth increases by increasing of the undepleted absorption layer then of the x_{au} is ~ *0.25 μm* the 3-dB bandwidth gradually decreases because the junction capacitance increase for thinner x_{ai}. ($x_{ai} = x_a - x_{au}$). This results is adopted to the experimental data from [1].

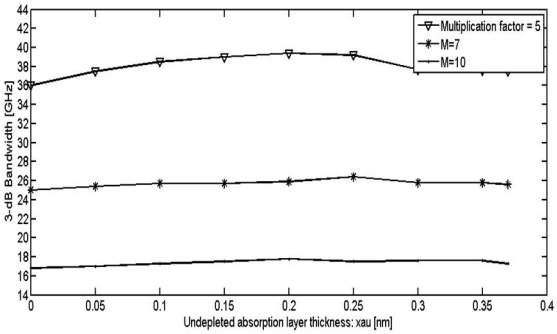

Fig.4. Theoretical 3-dB bandwidth as a function of undepleted layer thickness for different multiplication factors.

Fig.5. shows 3-dB bandwidth versus multiplication factor, when the undepleted absorption layer was introduced the 3-dB bandwidth is improved in the low multiplication factor range.

Fig.6. shows the effect of the thickness of the multiplication layer x_m. by increasing x_m because of the decrease of the photodetectors capacitance the 3-dB bandwidth increases.

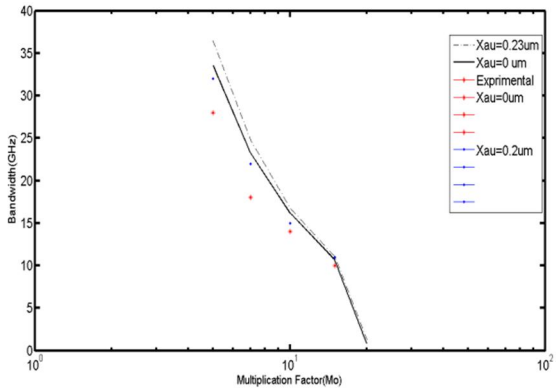

Fig.5. Theoretical results on 3-dB bandwidths as a function of multiplication factor for the WG-APD with the undepleted absorption layer (xau=0.2 μm) and without the undepleted absorption layer (xau=0μm)

Fig.6. Gain-bandwidth for WG-APD with different multiplication layer.

6. Conclusion

In this paper, we studied on the WG-APD with undepleted absorption layer that improve the 3-dB bandwidth without degrading responsibility by using the circuit model a new transfer function for this structure was presented.

The frequency and time responses where analysed that caused the gain-bandwidth characteristics where investigate. this undepleted absorption layer was effective in increasing the 3-dB bandwidth. Also the influence of thickness of the absorption and multiplication layer was illustrated for a multiplication factor of 7 the 3-dB bandwidth was obtained over 20Ghz.

By comparing this results against another photodetector, we conclude that the WG-APD with undepleted layer is appropriate for use in the high-speed long-haul communication.

Appendix:

secondary holes:

$$\frac{x_c + \Delta\omega_m}{v_n},$$

For o<t< no secondary holes are generated because no photogenerated primary carriers have reached the effective multiplication interface plane in the multiplication layer.

$$\frac{x_c + \Delta\omega_m}{v_n}$$

Then for o< t<

$$p_s(t) = o \qquad (1)$$

$$For \frac{x_c + \Delta\omega_m}{v_n} < t < \frac{x_{au} + x_{ai} + x_c + \Delta\omega}{v_n}$$

$$p_s(t) = N_o(M_o - 1)\left(\frac{v_n t - (x_c + \Delta\omega_m)}{x_a}\right) \otimes \left(\frac{\exp\left(-\frac{t}{(M_o - 1)\tau_m}\right)}{(M_o - 1)\tau_m}\right) \qquad (2)$$

$$\text{for} \frac{x_{au} + x_{ai} + x_c + \Delta\omega}{v_n} < t < \frac{x_c + \Delta\omega}{v_n} + \frac{x_{ai} + x_c + \Delta\omega}{v_P} + \frac{x_{au}}{v_{p1}}$$

The number of secondary holes will be

$$p_s(t) = N_o(M_O - 1) \otimes \left(\frac{\exp\left(-\frac{t}{(M_o - 1)\tau_m}\right)}{(M_o - 1)\tau_m}\right) \qquad (3)$$

$$for \frac{x_c + \Delta\omega}{v_n} + \frac{x_{ai} + x_c + \Delta\omega}{v_P} + \frac{x_{au}}{v_{p1}} < t <$$

$$\frac{x_{ai} + x_{an} + \Delta\omega_m + x_c}{v_n} + \frac{x_{ai} + x_c + \Delta\omega_m}{v_p} + \frac{x_{au}}{v_{p1}}$$

All secondary holes are generated. the number of the secondary holes at this time period is expressed as

$$P_s(t)=\eta(M_O-1)\frac{P_i}{h\nu} \qquad (4)$$

$$\times\left\{\left(\frac{v_n t-(x_c+\Delta\omega_m)}{x_a}\right)\times\right.$$

$$\left[u\left(t-\frac{x_c+\Delta\omega_m}{V_n}\right)-u\left(t-\frac{x_{au}+x_{ai}+x_c+\Delta\omega_m}{v_n}\right)\right]$$

$$+\left[u\left(t-\frac{x_{au}+x_{ai}+x_c+\Delta\omega_m}{V_n}\right)-u\left(t-\left(\frac{x_c+\Delta\omega_m}{v_n}+\frac{x_{ai}+x_c+\Delta\omega_m}{v_p}+\frac{x_{au}}{v_{p1}}\right)\right)\right]$$

After that, all secondary holes get collected in the p^+ contact layer. thus for

$$t>\frac{x_{ai}+x_{an}+\Delta\omega_m+x_c}{v_n}+\frac{x_{ai}+x_c+\Delta\omega_m}{v_p}+\frac{x_{au}}{v_{p1}}$$

The number of the secondary holes are zero. The number of the secondary holes as a function of time is expressed:

$$+\left(\frac{x_{au}\left(1+\frac{v_n}{v_{p1}}\right)+\left(x_{ai}+x_c+\Delta\omega_m\right)\left(1+\frac{v_n}{v_p}\right)-v_n t}{x_a}\right)$$

$$\times\left[u\left(t-\left(\frac{x_c+\Delta\omega_m}{v_n}+\frac{x_{ai}+x_c+\Delta\omega_m}{v_p}+\frac{x_{au}}{v_{p1}}\right)\right)-\right.$$

$$\left.u\left(t-\left(\frac{x_{ai}+x_{au}+\Delta\omega_m+x_c}{v_n}+\frac{x_{ai}+x_c+\Delta\omega_m}{v_p}\right)\right)\right]$$

$$\otimes\left\{\frac{\exp\left(-\frac{t}{(M_o-1)\tau_m}\right)}{(M_o-1)\tau_m}\right\} \qquad (5)$$

Corresponding Author:
S. Nikmanesh
School of Electrical and Computer Eng. Shiraz University
Email: nikmaneshsamira14@yahoo.com

References

1 J. C. Campbell, "Recent advances in telecommunications avalanche photodiodes," *J. Lightw. Technol.*, vol. 25, no. 1, pp. 109–121, Jan. 2007.
2 K. Kato and Y. Akatsu, "High-speed waveguide photodetectors," in *Proc. Int. Conf. InP Related Materials*, May 1995, pp. 349–352.
3 N. Lotfivand and H. Rasooli saghai, " A comparison of band width in RCE-SAGCM-APD and WG-SACM-APD structures, based on PSPICE model".
4 Y. Hirota, S. Ando, and T. Ishibashi, "High-speed avalanche photodiode with a neutral absorption layer for 1.55 um wavelength," *Jpn. J. Appl. Phys.*, vol. 43, no. 3A, pp. L375–L377, 2004.
5 N. Li, R. Sidhu, X. Li, F. Ma, X. Zheng, S. Wang, G. Karve, S. Demiguel, A. L. Holmes, Jr., and J. C. Campbell, "InGaAs/InAlAs avalanche photodiode with undepleted absorber," *Appl. Phys. Lett.*, vol. 82, no. 13, pp. 2175–2177, Mar. 2003.
6 J. E. Bowers and C. A. Burrus, "Ultrawide-band long-wavelength p-i-n photodetectors," *J. Lightw. Technol.*, vol. LT-5, no. 10, pp. 1339–1350, Oct. 1987.
7 T. Nakata, T. Takeuchi, K. Makita, Y. Amamiya, T. Kato, Y. Suzuki, and T. Torikai, "High-sensitivity 40-Gb/s receiver with a wideband In-AlAs waveguide avalanche photodiode," presented at the Eur. Conf. Optical Communications, Copenhagen, Denmark, 2002, Paper 10.5.1.
8 K. Shiba, T. Nakata, T. Takeuchi, T. Sasaki, and K. Makita, "10 Gbit/s asymmetric waveguide APD with high sensitivity of □□_ dBm," *Electron. Lett.*, vol. 42, no. 20, pp. 1177–1178, Sep. 2006.
9 T. Ishibashi, S. Kodama, N. Shimizu, and T. Furuta, "High-speed response of uni-traveling carrier photodiodes," *Jpn. J. Appl. Phys.*, vol. 36, no. 10, pt. Part 1, pp. 6263–6268, Oct. 1997.
10 S. S. Murtaza, K. A. Anselm, C. Hu, H. Nie, B. G. Streetman, and J. C. Campbell, "Resonant-Cavity Enhanced (RCE) Separate Absorption and Multiplication (SAM) Avalanche Photodetector (APD)," *IEEE Photon. Technol. Lett.*, vol. 7, no. 12, pp. 1486–1488, Dec. 1995.
11 [Online]. Available: http://www.cfp-msa.org/Apr. 1, 2010.
12 S. Shimizu, K. Shiba, T. Nakata, K. Kasahara, and K. Makita, "40 Gbit/s waveguide avalanche photodiodes with p-type absorption layer and thin InAlAs multiplication layer," *Electron. Lett.*, vol. 43, no. 8, pp. 476–477, Mar. 2007.
13 A. Alping, "Waveguide PIN Photodetectors: theoretical analysis and design criteria," *Proc. IEE Optoelectronics Conf.*, vol. 136, no. 3, pp.177–182, Jun. 1989.
14 W. Wu, A. R. Hawkins, and J. E. Bowers, "Frequency response of avalanche photodetectors with separate absorption and multiplication layers," *J. Lightw. Technol.*, vol. 14, no. 12, pp.

2778–2785, Dec. 1996.

15 D. Huber, R. Bauknecht, C. Bergamaschi, M. Bitter, A. Huber, T. Morf, A. Neiger, M. Rohner, I. Schnyder, V. Schwarz, and H. Jäckel, "In PIn Ga As single HBT technology for photoreceiver OEICs at 40 Gb/s and beyond," *J. Lightw. Technol.*, vol. 18, pp. 992–998, Jul. 2000.

16 K. Yang, A. L. Gutierrez-Aitken, X. Zhang, G. I. Haddad, and P. Bhattacharya,"Design, modeling, and characterization of monolithically integrated InP-based (1.55 _m) high-speed (24 Gb/s) p-in/HBT frontend photoreceivers," *J. Lightw. Technol.*, vol. 14, pp. 1831–1839, Aug. 1996.

17 Yasser M. EL-Batawy, student Member, IEEE, AND M. Jamal Deeen, Fellow, IEEE,"Analysis and circuit Modeling of Waveguide – separated absorption charge multiplication- avalanche photodetector (WG-SACM-APD)" IEEE transactions on electron Device, vol 52, No.3, march 2005.

18 Kazuhiro Shiba, Takeshi Nakata, Takeshi Takeuchi, Kenichi Kasahara, and Kikuo Makita, " Theoretical and Experimental Study on wave guide Avalanche photo diodes with an Undepleted Absorption layer for 25-Gb/s Operation", Journal of light wave technology, vol. 29/No.2, January 15,2011.

19 T. Nakata, I. Watanabe, K. Makita, and T. Torikai, "InAlAs avalanche photodiodes with very thin multiplication layer of 0.1 □m for highspeed and low-voltage-operation optical receiver," *Electron. Lett.*, vol. 36, no. 21, pp. 1807–1809, Oct. 2000.

20 T. Ishibashi, T. Furuta, "InP/InGaAs uni-traveling-carrier photodiodes," *IEICE Trans. Electron.*, vol. E-83-C, no. 6, pp. 938–949, Jun. 2000.

3/25/2020